OPEN ACCESS

LETTER

The Innovation Life

Mapping neuronal dynamics in the Thalamus underlying consciousness transition in macaques

Yueqi Wang,[1,2] Xinhe Liu,[2,3] Zhiting Zhang,[2,3] Panke Yu,[2,3] Ming Yin,[1,*] and Ji Dai[2,3,4,*]

[1]Key Laboratory of Biomedical Engineering of Hainan Province, One Health Institute, Hainan University, Haikou 570228, China

[2]Shenzhen Technological Research Center for Primate Translational Medicine, Shenzhen-Hong Kong Institute of Brain Science, Shenzhen Institutes of Advanced Technology, CAS, Shenzhen 518055, China

[3]Guangdong Provincial Key Laboratory of Brain Connectome and Behavior, Shenzhen Institutes of Advanced Technology, CAS, Shenzhen 518055, China

[4]University of Chinese Academy of Sciences, Beijing 100049, China

*Correspondence: ji.dai@siat.ac.cn (J.D.); ming_yin@hainanu.edu.cn (M.Y.)

Received: May 28, 2025; Accepted: August 12, 2025; Published Online: August 14, 2025; https://doi.org/10.59717/j.xinn-life.2025.100152

Citation: Wang Y., Liu X., Zhang Z., et al. (2025). Mapping neuronal dynamics in the Thalamus underlying consciousness transition in macaques. *The Innovation Life* **3**:100152.

Dear Editors,

Consciousness, defined as our subjective awareness of both ourselves and our environment, continues to be one of the most enigmatic challenges in the field of neuroscience.[1] While the specific neural correlates of consciousness remain largely undefined, accumulating evidence suggests that the thalamus serves as a vital center for its generation and sustenance.[2] This highly interconnected structure functions as an essential relay for sensory, motor, and limbic information, facilitating extensive communication with the cerebral cortex. Such complex interactions indicate that the thalamus is instrumental in integrating and modulating cortical activity, a process deemed crucial for the experience of consciousness.[3] Nevertheless, despite notable progress in elucidating the thalamus's role in consciousness, our comprehension of the dynamic neuronal processes involved in the transition from unconsciousness to consciousness is still quite limited. For instance, what mechanisms do thalamic neurons employ to facilitate the restoration of consciousness?

To address this critical gap, we investigate the neuronal activity within the thalamus of macaques during the recovery process from propofol-induced anesthesia, which is a well-established paradigm for consciousness studies.[4] The study aims to: (1) Characterize the temporal dynamics of neuronal firing rates during the emergence from unconsciousness. (2) Identify patterns of neuronal activity that correlate with specific stages of recovery, such as the return of responsiveness and the re-establishment of conscious awareness.

To this end, we continuously monitored the spiking activity of multiple thalamic neurons using in-*vivo* electrophysiological techniques (Figure 1A) while also tracking other physiological parameters, such as heart rate and electromyography (EMG).[5–7] For analytical purposes, we categorized the recovery process into four distinct states (see Figure 1B), informed by the physiological indicators and consciousness scoring.[8] The method rigorously assesses five distinct indicators—facial movements, eye movements, oral movements, limb and body movements, and vital signs—by assigning each a score of 0, 1, or 2. The cumulative total of these scores produces a final arousal score, which ranges from zero to ten.[8] State A signifies a baseline condition where the subjects remained under stable anesthesia, reflected by a consciousness score of zero (Figure 1C). Upon cessation of propofol administration, we entered State IR, initiating recovery; however, muscle activity remained dormant, indicating an early recovery phase. State LR was marked by a pronounced increase in heart rate, typically accompanied by bursts in EMG (Figure 1B), coupled with an elevation in arousal score (Figure 1C), characterizing the late recovery stage. Finally, in State RA, we re-induced anesthesia in the animal through propofol administration, representing a return to an anesthetic state.

OVERVIEW OF NEURONAL DYNAMICS DURING THE RECOVERY AND LOSS OF CONSCIOUSNESS

Following the delineation of these states, we engaged in comprehensive analyses to explore neuronal activity within them. A total of 570 well-isolated neurons recorded from seven macaques were included in the analysis. Utilizing dimensionality reduction approaches, we classified the neurons according to their waveform characteristics into four distinct clusters (Clusters 1, 2, 3, and 4, see Figure 1D).[6] We mapped the recording locations of these neurons along the dorsal-ventral axis (Figure 1E). Our analysis revealed that a greater proportion of Cluster 2 neurons were located dorsally (66.36% vs. 33.64%), while other clusters of neurons were more slightly concentrated in the ventral thalamus.

To investigate neuronal dynamics during the recovery from anesthesia, we constructed heat maps to illustrate the firing rates for all cell clusters across States IR to RA (Figure 1F). Notably, neurons of each cluster were arranged by their relative depth within the thalamus, with each row representing one neuron, mirroring the structure in Figure 1E. In State IR, approximately two minutes after stopping propofol, most neurons across all clusters began to exhibit increased activity, despite the absence of noticeable behavioral or physiological changes. This suggests that alterations in neuronal firing may serve as early indicators of consciousness recovery. The activity in State LR intensified significantly, particularly for Cluster 3 and 4 neurons, which exhibited a sharp rise concurrent with the heart rate increase (around 2 minutes into State LR). Cluster 3 neurons demonstrated a significant depth-dependent variation, characterized by robust activation in dorsal neurons, whereas central neurons exhibited erratic firing patterns. Similarly, Cluster 1 neurons located in the dorsal region displayed an activation pattern akin to that of Cluster 3. In contrast, the ventral portion of Cluster 1 neurons, along with Cluster 2 neurons, exhibited more subdued increases that occurred at an earlier stage. In State RA, after reintroducing propofol, the majority of neurons reverted to silence. Interestingly, some neurons maintained heightened activity even as the subjects became re-anesthetized.

To further delineate response characteristics, we generated mean response curves in different states for all cell clusters (Figures 1G-I). Although all four clusters exhibited similar responses during States IR and RA, substantial differences were evident in State LR. To quantify these disparities, we identified the steepest points on the curves, signaling the most rapid changes during State LR. Specifically, Cluster 1, 2, and 4 neurons peaked at 106, 114, and 116 seconds, respectively, while Cluster 3 neurons showed a profoundly delayed peak at 158 seconds (Figure 1H). This temporal discrepancy aligns with the patterns observed in the heat maps, highlighting asynchronous activation and cell-type-dependent variations in the neuronal recovery sequences.

PERSISTENCE OF NEURONAL ACTIVATION AMIDST LOSS OF CONSCIOUSNESS

In State RA, we noted a significant phenomenon in which specific neurons maintained their firing rates rather than experiencing a decline after the re-administration of anesthetics. Remarkably, some of these neurons even exhibited a notable increase in their activity. To investigate this fascinating observation in greater depth, we initially identified the neurons that were actively firing by comparing their firing rates during the last three minutes to those in the first minute. We then proceeded to map the variations in firing rates for both the active (Figure 1J) and inactive groups (Figure 1K).

Our analysis revealed that Cluster 3 neurons constituted the highest proportion of active cells in State RA, accounting for an impressive 27.11%. In contrast, Cluster 1, Cluster 2, and Cluster 4 neurons made up 24.20%, 23.81%, and 17.83%, respectively. Among the actively firing neurons, we observed that Cluster 1 and Cluster 3 neurons reached distinct firing peaks at about 80 and 100 seconds, respectively, following propofol administration. In contrast, Cluster 2 and Cluster 4 neurons tended to maintain consistent activation

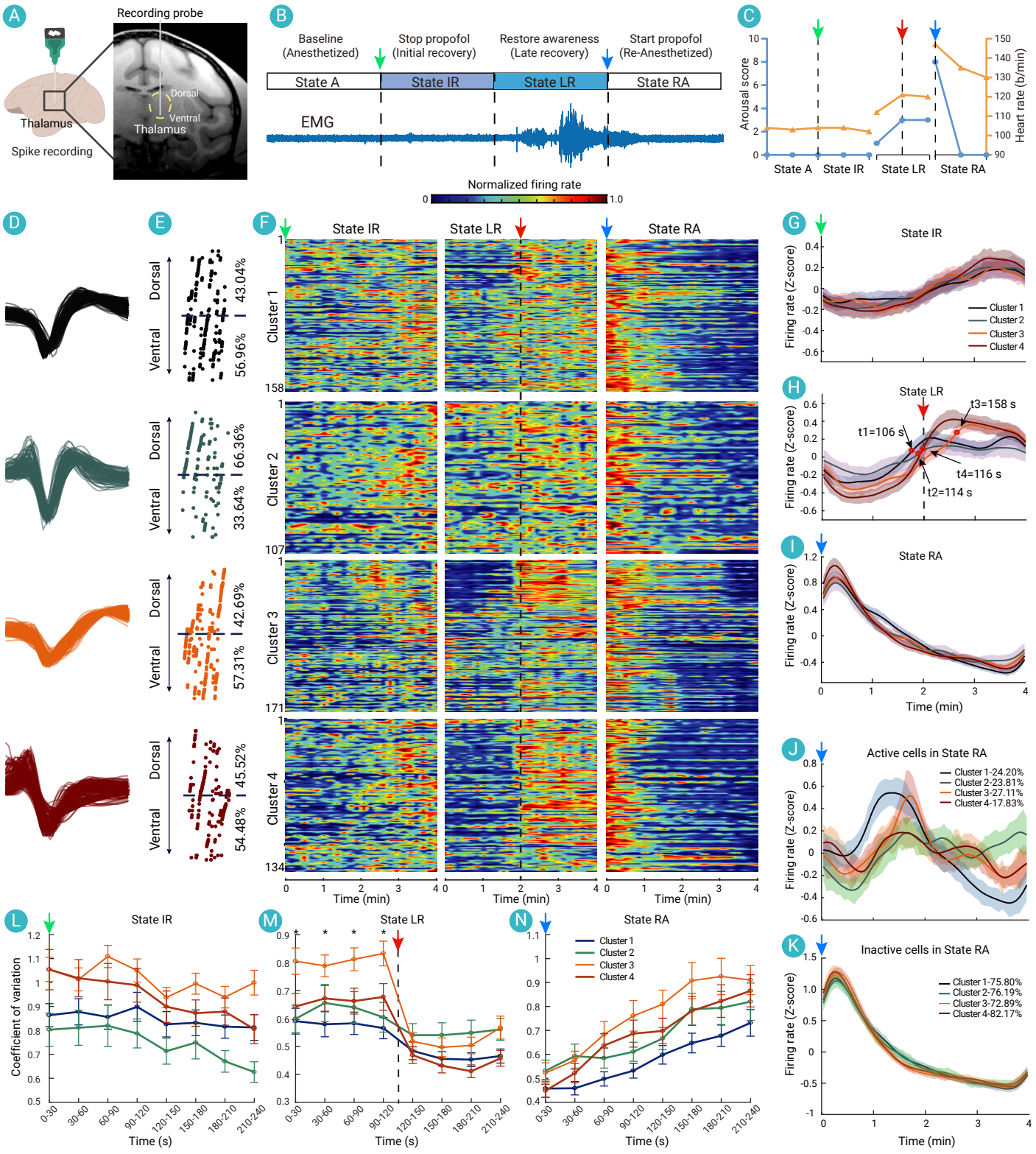

Figure 1. Mapping Neuronal Dynamics in the Thalamus Underlying Consciousness Transition in Macaques (A) The locations of recordings within the thalamus, accompanied by a schematic of the recording probe. (B-C) Four distinct states are identified: baseline (State A), Initial recovery (State IR), late recovery (State LR), and re-anesthetized (State RA), determined through the evaluation of arousal levels. The blue trace in (B) represents a sample of the EMG recording, the yellow line in (C) represents the recording of heart rate, and the blue line represents the arousal score. Green arrows: the cessation of propofol; blue arrow: the initiation of propofol; red arrow: the abrupt rise in arousal score during the late recovery phase. (D) Classification of neurons into four distinct clusters based on their spike waveforms. (E) Representation of the distribution of dorsal and ventral thalamus neurons corresponding to the four clusters. (F) Heat maps illustrating the firing dynamics of each neuron cluster across States IR, LR, and RA. Each row in these maps represents one neuron and is arranged by its relative depth in the thalamus. The color bar indicates the normalized firing rate. The dashed line aligns with the red arrow. (G-I) Average firing rates for the different neuron clusters in States IR, LR, and RA, with the dots in State LR marking the time point of the most rapid increase for each cluster. The shaded regions represent the standard error. (J and K) The Z-scored averaged firing rates of active neurons and inactive neurons in State RA. The legends on the right provide information about neuron clusters along with the percentage of active or inactive neurons within each category. The shaded regions represent the standard error. (L-N) The CV measurements for various neuron clusters in States IR, LR, and RA, are presented respectively. Error bars denote standard error. $*p < 0.05$.

levels well beyond one minute (Figure 1J). This divergence underscores the functional distinctions between these neuronal clusters during the transitional phases of anesthesia.

In stark contrast, the inactive neurons displayed remarkably similar firing patterns, characterized by a steady decline in activity following the re-administration of propofol (Figure 1K). This reduction in firing underscores the profound suppressive effects of anesthesia on neuronal populations, indicating that a majority of neurons, irrespective of cluster, were effectively inhibited to achieve the desired anesthetic state.

VARIATIONS IN NEURONAL ACTIVITY DURING THE RECOVERY PROCESS

To further evaluate the variations in neuronal activity during the recovery process, we meticulously analyzed the coefficient of variation (CV) of spiking activity for each neuron cluster across each state (Figures 1L-N). The CV serves as a statistical measure that represents the size of the standard deviation (STD) relative to the mean of the neuronal firing rates (CV = STD of firing rate / Mean firing rate). A small CV typically indicates a high degree of consistency among signal emissions, suggesting stable and reliable neuronal firing patterns.[9] Here, CV values were determined for each 30-second window throughout the 4-minute recording period within each state for every individual cell. Subsequently, the averaged CVs across cells produced eight bins for each cell cluster in each state.

Our analysis revealed that thalamic neurons exhibited a decline in CV over time in both State IR and State LR ($p < 0.001$, Friedman test), irrespective of the cell clusters involved. This finding suggests that the restoration of consciousness is associated with reduced variability in neuronal firing patterns. Among the different cell clusters, Cluster 1 and Cluster 2 neurons generally showed the least variations, while Cluster 3 neurons consistently displayed the highest CV across all states. Notably, Cluster 3 neurons experienced a significant and sudden drop in CV following an increase in heart rate and consciousness score during State LR (Figure 1M), despite a substantial rise in their firing rates (Figure 1F). A repeated measures two-way ANOVA (Time × Cluster) demonstrated a significant main effect of Cluster on CV (Interaction: $F(8.560, 1545) = 0.971$, $p = 0.460$; Time: $F(3, 1545) = 0.449$, $p = 0.718$; Cluster: $F(3, 515) = 5.952$, $p < 0.001$). Subsequent Bonferroni post-hoc tests revealed that CVs in Cluster 3 were significantly greater than those in other clusters during the first 120 seconds ($p < 0.05$); however, this difference diminished after the consciousness score increased. This suggests that enhanced stability and regularity among spiking activities may be essential for individuals striving to regain consciousness, with Cluster 3 neurons appearing to play a critical role in the recovery process.

Moreover, after the administration of re-anesthesia, all observed CVs increased once more (Figure 1N), indicating a resurgence in variability across different neuronal populations within the anesthesia state. This heightened variation suggests a complex interplay in the neural circuits as they adapt to changes in physiological states. Overall, these findings underscore the significance of neuronal variability and synchronization in the context of consciousness recovery, highlighting the pivotal roles that specific neuronal clusters play in these critical processes.

CONCLUSION AND DISCUSSION

In this study, we identified four distinct clusters of neurons within the thalamus and analyzed their activity patterns during the phases of consciousness loss and subsequent recovery induced by propofol anesthesia, offering significant insights into the electrophysiological characteristics of various neuronal subtypes in the thalamus as it recovers from anesthesia.

Our findings underscore the critical role of Cluster 3 neurons in the process of regaining consciousness and sustaining anesthesia. Characterized by glutamatergic neuron-specific broad and slow-decaying spikes, these neurons are likely thalamocortical projection neurons, serving as the primary output neurons of the thalamus with projections to multiple cortical areas. The observation that a subset of cells remains activated during re-anesthesia and exhibits unique response patterns is particularly noteworthy. Further investigation is essential to fully understand the functional roles of these diverse neuronal subtypes and their contributions to the intricate dynamics of thalamocortical networks.

Future studies should employ a comprehensive approach that combines electrophysiological recordings with immunohistochemical staining for neurotransmitter markers, anatomical tracing techniques, and circuit-level manipulations. This will deepen our understanding of the diversity of thalamic neurons, specific roles of different thalamic nuclei, and their implications for anesthesia recovery. Additionally, a crucial area for future research involves clarifying the specific neural mechanisms that lead to the asymmetric patterns observed during the loss and recovery of consciousness. This may require a blend of electrophysiological studies, neuroimaging techniques, and computational modeling to gain a more nuanced understanding of how anesthesia influences brain network dynamics.[10] By exploring the mechanisms underlying the asymmetries in consciousness loss and recovery, we can uncover vital insights into the neural basis of consciousness and develop more effective strategies for managing anesthesia and addressing consciousness-related disorders.

REFERENCES

1. Shan L., Huang H., Zhang Z., et al. (2022). Mapping the emergence of visual consciousness in the human brain via brain-wide intracranial electrophysiology. *The Innovation* **3**:100243. DOI:10.1016/j.xinn.2022.100243
2. Wang H., Hu Y., Ge Q., et al. (2025). Thalamic burst and tonic firing selectively indicate patients' consciousness level and recovery. *The Innovation*:100846. DOI:10.1016/j.xinn.2025.100846
3. Ward L. (2011). The thalamic dynamic core theory of conscious experience. *Conscious Cogn.* **20**:464–486. DOI:10.1016/j.concog.2011.01.007
4. Mashour G. A. (2024). Anesthesia and the neurobiology of consciousness. *Neuron* **112**:1553–1567. DOI:10.1016/j.neuron.2024.03.002
5. Chen Y., Hong Z., Wang J., et al. (2023). Circuit-specific gene therapy reverses core symptoms in a primate Parkinson's disease model. *Cell* **186**:5394-5410 e5318. DOI:10.1016/j.cell.2023.10.004
6. Liu X., Zhang Z., Gan L., et al. (2025). Medium Spiny Neurons Mediate Timing Perception in Coordination with Prefrontal Neurons in Primates. *Adv Sci (Weinh)* **12**:e2412963. DOI:10.1002/advs.202412963
7. Zhang Z., Shan L., Wang Y., et al. (2023). Primate preoptic neurons drive hypothermia and cold defense. *The Innovation* **4**:100358. DOI:10.1016/j.xinn.2022.100358
8. Zhang Z., Huang Y., Chen X., et al. (2024). State-specific Regulation of Electrical Stimulation in the Intralaminar Thalamus of Macaque Monkeys: Network and Transcriptional Insights into Arousal. *Adv Sci (Weinh)* **11**:e2402718. DOI:10.1002/advs.202402718
9. Ditlevsen S. and Lánský P. (2011). Firing Variability Is Higher than Deduced from the Empirical Coefficient of Variation. *Neural Comput.* **23**:1944–1966. DOI:10.1162/NECO_a_00157
10. Feng G., Xu H., Wan S., et al. (2024). Twelve practical recommendations for developing and applying clinical predictive models. *Innov. Med.* **2**:100105. DOI:10.59717/j.xinn-med.2024.100105

FUNDING AND ACKNOWLEDGMENTS

The study was funded by the National Natural Science Foundation of China (32371066), the National Key R&D Program of China (2024YFF1206400), the Shenzhen-Hong Kong Institute of Brain Science–Shenzhen Fundamental Research Institutions (NYKFKT2019009), and Shenzhen Technological Research Center for Primate Translational Medicine (XMHT20220104005). The funders had no role in study design, data collection and analysis, decision to publish, or preparation of the manuscript.

AUTHOR CONTRIBUTIONS

J.D designed the experiment; Y.W, Z.Z. and P.Y collected the data; Y.W, X.L and J.D performed the analysis; Y.W and J.D wrote the manuscript. M.Y and J.D supervised the project. All authors contributed to the manuscript and approved the final version.

DECLARATION OF INTERESTS

The authors declare no competing interests.

ETHICAL STATEMENT AND PATIENT CONSENT

The study was approved by the Institutional Animal Care and Use Committee (IACUC) at the Shenzhen Institutes of Advanced Technology, Chinese Academy of Sciences (Approval Number: SIAT-IACUC-201014-NS-DJ-A0808-02).

DATA AND CODE AVAILABILITY

Data are available from the corresponding author upon reasonable request.